scientific reports

Check for updates

OPEN

# Development of an electrical current stimulator for controlling biohybrid machines

Riccardo Collu[1]✉, Judith Fuentes[2], Florencia Lezcano[2], Maria Crespo-Cuadraro[2], Andrea Bartolucci[3], Leonardo Ricotti[3], Lorenzo Vannozzi[3], Samuel Sánchez[2,4], Stefano Lai[1] & Massimo Barbaro[1]

**Soft and flexible robotics is an emerging field that attracts a huge interest due to its ability to produce bioinspired devices that are easily adaptable to the environment. Biohybrid Machines (BHM) represent a category of soft robots that integrate biological tissues, such as engineered muscle tissues, as actuating systems. Although these devices present several advantages in some applications, their proper actuation still represents a challenge for researchers. This paper focuses on the development of a portable and programmable electrical stimulator designed to control muscle fiber-based biohybrid actuators. The stimulator, made using off-the-shelf components, was designed as a stacking of three independent printed circuit boards (PCBs), connected vertically in order to result in a final device with compact dimensions of 59 mm × 28 mm × 25 mm. The stimulation circuit is capable of delivering currents up to 18 mA with a voltage compliance of ± 90 V, and a power consumption of approximately 1.3 W. The device's ability to induce twitch and tetanic contractions in a biohybrid actuator is demonstrated in different stimulation conditions. A practical application was also explored through a test case involving a flexible catheter prototype controlled by a biohybrid actuator, demonstrating its potential utility in a BHMs.**

**Keywords** Electrical current stimulator, Soft robotics, Biohybrid machines

Soft robots are attracting considerable interest due to their unique mechanical properties, which stem from the use of flexible, lightweight, and biocompatible materials. Biohybrid Machines (BHM) are a category of soft robots in which biohybrid actuators (i.e., living cells and tissues combined with artificial elements) are used to provide robot movement[1,2]. BHMs find their application in several fields, such as surgery and prosthetics, where typical soft robotic actuation methods (e.g., pneumatic) are not possible or inconvenient. Ricotti et al. identified two categories of biohybrid actuators based on their scalability and use: (1) application-oriented actuators or non-scalable devices, based mainly on the use of bacteria, motile cells, and devices based on explanted whole-muscle tissues; (2) general purpose actuators or scalable devices, based on the use of self-contractile tissues and engineered skeletal muscle tissues[2]. The latest category guarantees larger actuation forces, even in the hundreds of $\mu$N range, which is suitable for soft robotic applications.

In this sense, providing an effective actuation of tissue actuators becomes fundamental to the correct functionality of the soft robot[2]. Several approaches have been reported in the literature, including magnetic[3], optical[4,5], chemical, and electrical stimulation[6–8]. Magnetic stimulation has been proven to be capable of guiding the locomotion of biohybrid robots, in particular microorganism-actuated ones[9,10], anyway the control strategies typically require complicated equipment and algorithms[11]. Despite optical control allowing for the modulation of the contractile response of the biohybrid actuator[12], its main limitations lie in the limited adjustable stimulation parameters (i.e., amplitude, frequency, and pulse width), the need to genetically modify the living tissue to activate biohybrid actuators through light[13–15], and environmental restrictions. Light cannot be used in all kinds of environment as it cannot penetrate tissues and is difficult to employ in specific contexts, such as endoscopic or surgical applications.

In this sense, electrical stimulation represents a convenient strategy for muscle tissue control; nevertheless, the application of electrical signals can be potentially disruptive for the biohybrid actuator (e.g., causing the

[1]Department of Electrical and Electronic Engineering, University of Cagliari, 090123 Cagliari, Italy. [2]Institute for Bioengineering (IBEC), Barcellona, Spain. [3]The BioRobotics Institute, Scuola Superiore Sant'Anna, 56127 Pisa, Italy. [4]Institució Catalana de Recerca i Estudis Avançats (ICREA), Passeig de Lluís Companys 23, 08010 Barcelona, Spain. ✉email: riccardo.collu@unica.it

formation of toxic reagents within the stimulation environment and damaging the cells of living tissue), thus making the correct setting of the stimulation parameters (e.g., the stimulation waveform used, its amplitude, duration, and frequency) fundamental.[2,15]

In BHMs, electrical stimulation is generally performed in a Voltage Control Mode (VCM), i.e., by imposing a known potential drop between stimulation electrodes. For example, Cvetkovic et al. and Pagan-Diaz et al. have used biphasic stimuli up to 20 V and 50 ms of pulse width, using a waveform generator and an AD797 inverting amplifier connected to a capacitor, achieving stimulation frequencies up to 10 Hz[16,17]. In Filippi et al., the authors realized a closed-loop system to control a biohybrid actuator, where a bench waveform generator was employed to deliver 20 V pulses[8]. In Guix et al., the authors employed a bench waveform generator (PM8572, Tabor Electronics) connected to a signal amplifier (Model 9200, Tabor Electronics) to provide 15 V monophasic stimuli with frequencies up to 15 Hz[18]. Although several examples have thus been reported in the literature, many open challenges need to be addressed in BHM stimulation. First, VCM does not guarantee precise control over the charge injected during stimulation[19]. The injected current, and consequently the charge, depends on the load impedance, which is a function of several factors such as culture medium, the relative distance between the electrodes, their geometrical properties, and electrode oxidation. This limits the capability to predict the current and the charge used during the stimulation tasks, avoiding the possibility of comparing the results of the literature.

Second, the effectiveness of VCM is strongly reliant on the impedance of stimulation electrodes, which affects design scalability with the BHM dimensions. Aside from these limitations, some fundamental aspects are still barely explored. To date, little attention has been paid to the development of customized stimulation systems, adopting experimental setups that make use of one or multiple benchtop instruments responsible for stimulating tissues. Consequently, the programmability of stimulation signal features has been barely considered so far, although this aspect is crucial for developing effective control strategies.

In this paper, a circuit for the stimulation of biohybrid actuators through programmable current stimuli based on Current Control Mode (CCM) is reported. CCM allows for a more effective approach for precise control over the charge used during stimulation since the stimulation is provided by fixing the current flowing between electrodes. This approach limits the formation of toxic reagents due to the hydrolysis of the electrolytic solution that ensures the sustenance of bioactuators[19]. Although the development of current stimulators is well documented in sensory feedback and neural stimulation applications[20–23], the employment of the CCM approach in soft robotics is unprecedented. The proposed circuit is implemented in a modular, portable instrument, assembled by custom printed circuit boards (PCBs) and entirely fabricated using off-the-shelf components. The system ensures a high degree of programmability of electrical stimuli, in terms of amplitude, frequency, and pulse width to allow the development of advanced control techniques for biohybrid actuators based on muscle tissues. This feature aims not only at studying how to elicit different functions in the muscle actuator (e.g., twitch and tetanic contraction), but also the ability to modulate muscle fiber recruitment. To investigate these features, the proposed device was tested in different benchmarks, such as biohybrid actuators composed by C2C12, 3D-bioengineered muscle tissues and flexible supports, and a BHM using this actuator, i.e. a proof-of-concept prototype of a catheter tip with electrically-induced bendability.

## Methods

### Voltage and current controlled stimulation

When an excitable tissue is electrically actuated, a charge Q is injected through the tissue depending on the electric current that flows between stimulation electrodes, $I(t)$, following the equation[24]:

$$Q = \int I_{stim}(t)dt \tag{1}$$

In VCM stimulation, $I(t)$ is fixed by applying a voltage generator between the electrodes[19]. Due to Ohm's law, the current injected during stimulation is thus given by:

$$I(t) = V(t)/Z(t) \tag{2}$$

where $V(t)$ is the voltage applied by the voltage source, while $Z(t)$ is the impedance of the system composed of the stimulation electrodes and the electrolyte. In general, this impedance can be modeled by an equivalent RC circuit, which describes the interface between the electrodes and the electrolyte, as well as the behavior of ionic transport within the electrolyte[19,25]. These components may vary during experiments due to reactions in the proximity of the electrodes or changes in the electrolyte composition due to the metabolic reactions of the biological tissue used as actuator[19,26]. The dependence of injected current to $Z(t)$ in VCM may represents a serious issue in the controllability of the biohybrid actuator: an increase in impedance anywhere in the electrical path would lead to an additional voltage drop, causing a reduction of current and so a reduction in injected charge, which could become insufficient for stimulation. Moreover, since $Z(t)$ varies with geometrical dimensions in the system (e.g., electrodes area and relative distance)[27,28], stimulation conditions in VCM cannot be directly scaled: for instance, the passage to a miniaturized BHM can be related to an overall decrease of the impedance, and the same voltage source can thus provide an higher current[22,23], contributing to damaging the muscle tissue or to undesired side reactions, such as electrolysis of the media.

In CCM, stimulation is performed by connecting a current source between the electrodes. The current is therefore imposed by the circuit, and so it is the amount of charge injected, as this is independent of the impedance of the electrode-electrode system, as shown in Fig. 1, thus making control of the experimental conditions, and scaling to different BHM dimensions more straightforward. As a matter of fact, CCM is widely used in the field

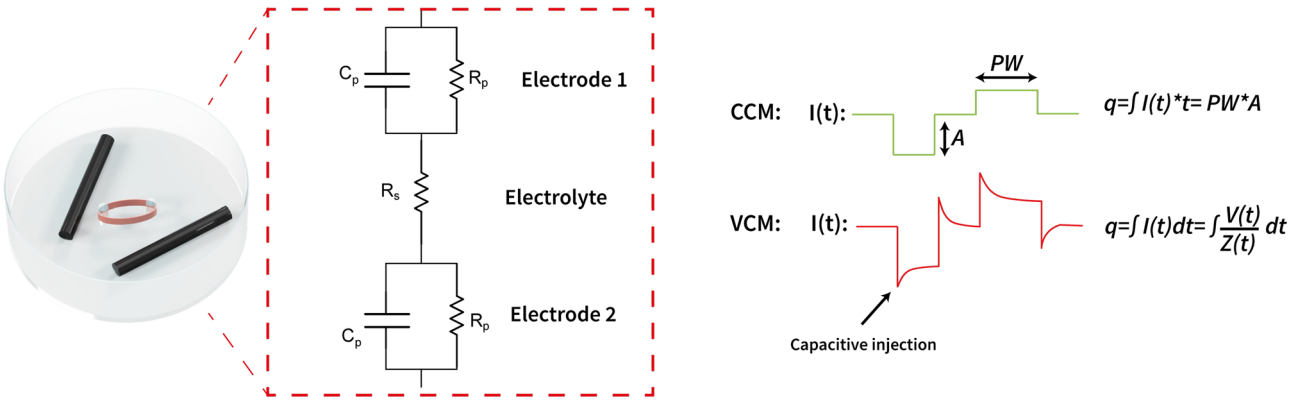


**Figure 1**. The impedance of the electrodes-electrolyte system can be described using an RC equivalent circuit. The contact impedance between the electrodes and the electrolyte is described using a parallel of a capacitor $C_p$ and a resistor $R_p$, while the impedance of the electrolyte between the electrodes is modeled using a pure resistor $R_s$. In VCM, the injected charge depends on the impedance, and due to the capacitive behaviour of the system this leads to some undesired overshoots and reduce scalability of the stimulation conditions with BHM dimensions. In CCM the injection of charge does not depend on the impedance but only on the current imposed by the current source.

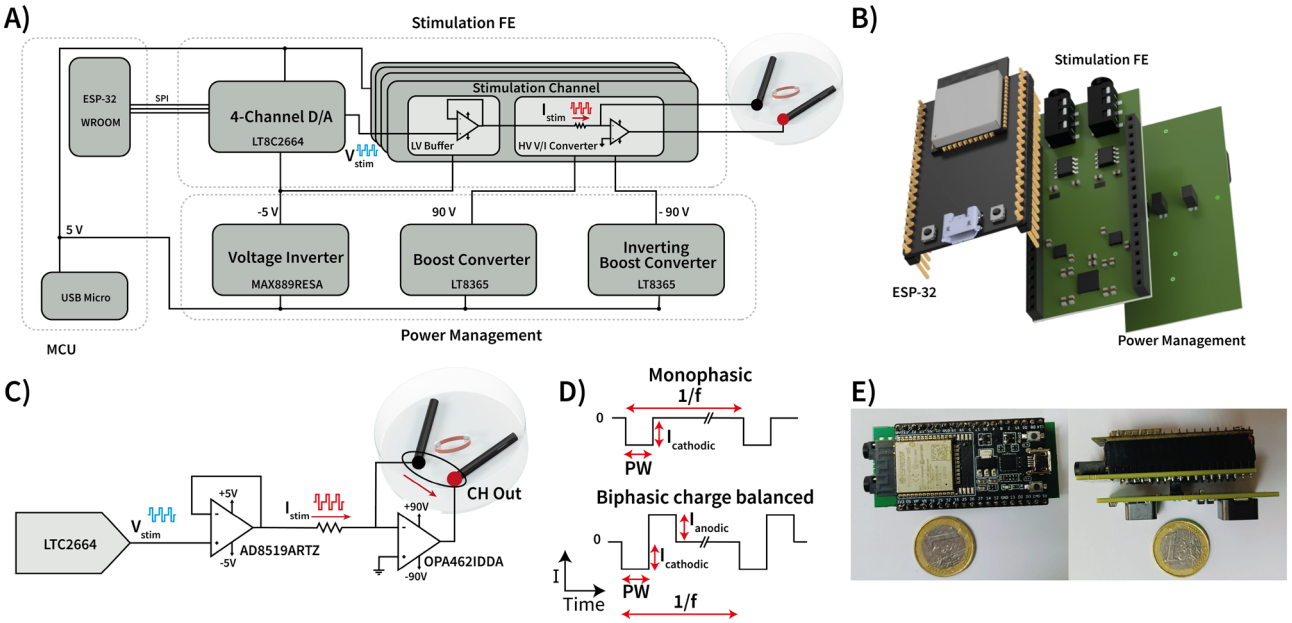


**Figure 2**. The current stimulator developed in this study designed the stacking of two custom PCBs for power supply and stimulation unit (**A**). The Power management unit generates the voltages required by the stimulation Front-End (FE). The stimulation FE is composed of four different voltage-to-current converters used to stimulate the biohybrid actuators. The simulator has been realized as a stacked system (**B**). The stimulation channel is based on a voltage-controlled voltage-to-current converter (**C**). The programmability of the stimulation FE allows the customization of the stimuli in terms of shape, pulse width (PW), frequency (f), and current amplitude (I) (**D**). Images of the final device in front and lateral view (**E**).

of electrical stimulation on humans, as this makes the stimulation system safer, avoiding injections of capacitive charge that could alter the balance of stimulation and consequently lead to potential adverse reactions in the nearness of the electrodes. The system we designed applies these principles, aiming to guarantee safe stimulation protocols. With this in mind, the stimulation system is one of the building blocks of a future complete system based on biohybrid actuators.

## Electronic stimulator

Figure 2 shows the configuration of the proposed stimulator: in order to keep dimensions feasible for a portable stimulator system, the developed circuit is configured as a 59 mm × 28 mm × 25 mm (L × W × H) stacked

system, composed of two custom PCBs and a commercial microcontroller unit. This approach separates the power management units and the stimulation front-end (FE), resulting in a modular device that can be easily modified in terms of voltage compliance and stimulation current characteristics. Each PCB is a 59 mm × 28 mm, two-layer board designed to be mounted (the same size, the same profile) on the commercial development microcontroller unit (MCU) board ESP32-WROOM-32UE, a dual-core 32-bit microprocessor with a built-in Bluetooth module and USB peripheral.

The power management unit is located on the bottom of the stack, and it is used to generate the supply voltages required by the stimulation front-end. It contains two booster circuits based on the switching voltage regulators Analog Devices Inc. (Wilmington, MA, USA) LT8365 and a voltage-inverting circuit. The voltage inverting circuit is based on Maxim Integrated (San Jose, CA, USA) MAX889RESA, which allows the generation of -5 V used by the front-end, a current of 200 mA with a quiescent current of 2 mA. The LT8365 is a voltage converter employed in boosting or inverting voltages, which guarantees a low quiescent current and low ripple on the output. The LT8365 has been used in two different circuits. The first one exploits the boosting feature of the component, allowing a 90 V voltage supply starting from the 5 V input supply, with a maximum current delivered to the load up to 66 mA. The second circuit uses the inverting feature of the LT8365 to generate a -90 V voltage supply from the 5 V input supply. The high voltage compliance (± 90 V) guaranteed by the power management module has been designed to adapt the stimulator to a maximum load of 5 kOhm, thus ensuring a wide margin of investigation in the choice of electrodes and electrolytic media required.

The FE unit is located in the middle of the stack; it takes the high-voltage bipolar supply from the power management unit and the 5 V supply from the MCU. It hosts a 4-channel 16-bit bipolar digital-to-analog converter (DAC), Analog Devices LTC2664, connected to the four different stimulating channels. Each output channel is a voltage-programmable voltage-to-current converter that delivers the current to the load employing two amplifiers, a low voltage rail-to-rail amplifier Analog devices (Massachusetts, USA) AD8519ARTZ and high voltage Texas Instruments (Dallas, Texas, USA) OPA462IDDA, as reported in Fig. 3.

The MCU uses the SPI protocol to program the DAC, allowing users to turn ON or OFF any of the four channels. The low voltage amplifier acts as a buffer to sink/source the stimulation current whose value is set by the DAC output voltage and resistor $R_{stim}$. The load requiring stimulation is connected in feedback to the high-voltage amplifier, ensuring the $I_{stim}$ current flow as described in[23]:

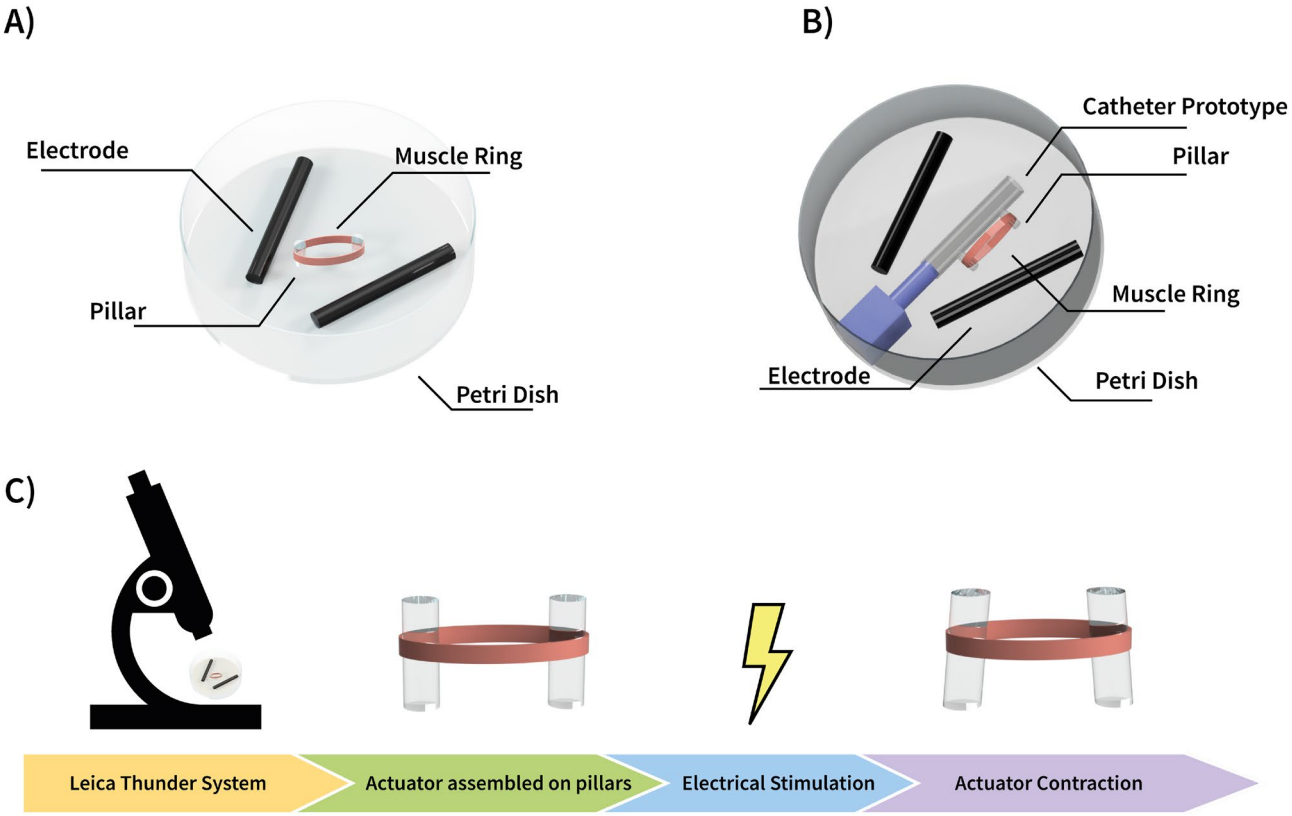


**Figure 3**. Measurement setup. Tissues were assembled on two different Petri Dish. On the first Petri dish, the actuator was assembled on two PDMS pillars built on the bottom of the Petri, while electrical stimulation was provided using two graphite electrodes (**A**). The second Petri dish contained a catheter prototype. The muscle ring actuator was mounted on the catheter (**B**). During the measurements, the Petri dish was observed using the Leica Thunder System recording the tissue contractions induced by the electrical stimulation (**C**).

$$I_{stim} = \frac{V_{DAC}}{R_{stim}} \tag{3}$$

In this way, since the value of the applied current is independent from the impedance of the load, the total charge injected through monophasic or biphasic stimulation into the load is known:

$$Q = I_{stim} * PW \tag{4}$$

In the latter, Q is the injected charge and PW is the pulse width of the stimulation waveform. To ensure correct load stimulation, the OPA462IDDA amplifier adjusts its output voltage within the wide range provided by the ±90 V supply. OPA462IDDA ensures a slew rate of 32 V/$\mu$s and a maximum output current of about ±45 mA.

The LTC2664 DAC is equipped with an internal reference voltage that can be programmed in the range of ±2.5 V and ±5 V, thus allowing 381 nA current resolution in the range of 0-12.5 mA and 762 nA from 12.5 mA to 18 mA. The DAC guarantees the generation of a maximum of 2 ksps, thus allowing stimulation pattern shapes with frequencies higher than those required for tetanic contraction, typically lower than 100 Hz[29,30]. The programmability range of electrical stimuli, in terms of amplitude, frequency, and pulse width, is reported in Table 1.

## Control software and GUI

The full programmability of the proposed device allows for stimulation with arbitrary waveforms, including both monophasic or biphasic stimuli, typically used for Functional Electrical Stimulation (FES) or Nerve Electrical Stimulation (NES) on humans[31]. Although the use of the monophasic form is among the most used in the field of electrical stimulation, continuous exposure to a sequence of monophasic pulses could potentially induce damage to the tissue due to irreversible chemical reactions near the electrodes, giving rise to toxic products for the tissues[32]. On the contrary, the employment of biphasic pulses may mitigate such risks, as the reverse electric field generated by the subsequent positive phase of a biphasic pulse may impede the accumulation of cations/anions, thus preventing irreversible chemical reactions near electrodes[19,32,33]. For this reason, the device has been programmed with four default stimulation waveforms based on monophasic and biphasic shapes (monophasic, symmetric biphasic, charge-balanced asymmetric biphasic, and symmetric triangular), which can be modified in terms of frequency, pulse width (PW), and amplitude through a custom Matlab Graphical User Interface (GUI). In particular, PW can be tuned from 200 $\mu$s up to 60 ms in steps of 100 $\mu$s, the frequency from 1 Hz up to 500 Hz in steps of 1 Hz, and the amplitude from 0 to 18 mA in steps of 100 $\mu$A. Through the GUI, the user can also generate specific stimulation algorithms based on linear modulation of amplitude, frequency, or PW. Amplitude and frequency modulation can also be implemented using linear steps or via a trapezoidal pattern to allow the possibility of advanced control strategy investigation that is useful in adapting the stimulation to the different biological tissues used as actuators.

## Biohybrid actuator fabrication

The fabrication of the skeletal muscle-based actuators was done following the protocol reported in Guix et al.[18]. Briefly, C2C12 mouse myoblasts were purchased from ATCC (CRL-1772) and cultured in flasks until 80% confluence, at 37 °C and 5% CO2, in growth media (GM), which consist of high-glucose Dulbecco's modified Eagle's medium (DMEM; Gibco) supplemented with 10% fetal bovine serum (Gibco), 200 nM l-glutamine (Gibco), and 1% penicillin-streptomycin (Gibco). Once cells reached confluency, they were trypsinized and mixed with the hydrogel mix composed of 30% v/v of Matrigel (Corning), 4 U/mL of thrombin (Sigma-Aldrich), 4 mg/mL of fibrinogen (Sigma-Aldrich) and 10 million/ml of C2C12 cells. The 3D cell-laden hydrogel was cast in a circular mold made of PDMS, which was previously 3D printed, cured, sterilized under UV light, and treated with pluronic acid to avoid cell attachment. Cells were cultured in the hydrogel mix for 2 days in GM supplemented with 1 mg/ml 6-aminocaproic acid (ACA, Sigma-Aldrich) to avoid hydrogel degradation by cell protease. After this culture time, cell-laden hydrogels were gently removed from the circular molds and transferred to a flexible PDMS-based two-post system, where they were cultured in differentiation media (DM) until the day of experiments (days 10-11 of differentiation). DM consists of DMEM containing 10% horse serum (Gibco), 200 nM l-glutamine (Gibco), 1% penicillin-streptomycin (Gibco), 50 ng/ml IGF-1 (Sigma-Aldrich), and 1 mg/ml ACA.

## Flexible catheters fabrication

Custom-made catheters as prototypes of a biohybrid machine were fabricated using molds designed in Autodesk Fusion and manufactured through stereolithography (SLA) (Form 3B+, FormLabs) with Surgical Guide Resin to improve surface finish and quality. The molds were composed of four main components and a metal plug designed to fabricate a catheter with an internal diameter of 1.2 mm and a wall thickness of 500 $\mu$m. A

| Parameter | Min | Max | Step |
|---|---|---|---|
| Amplitude | 0 mA | 18 mA | 381–762 nA |
| Frequency | 1 Hz | 500 Hz | 1 Hz |
| Pulse width | 100 $\mu$s | 50 ms | 20 $\mu$s |

**Table 1**. Programmability range.

representation of the molds is shown in Supplementary Material Figure 1S. The base included concentric holes for aligning the plug, allowing material flow to define wall thickness and two lateral holes for material injection. Two lateral components enclosed the plug, featuring semi-circular cavities that matched the catheter's external radius, with one of the pieces including holes specifically designed for pillar fabrication. Pillars with a diameter of 1 mm and a height of 1.5 mm were fabricated at a distance of 9 mm to provide an anchoring site for the biohybrid actuator. The catheter bending was enabled upon the electrical stimulation of the biohybrid actuator. The upper component resembled the base, with similar holes for screws, alignment, and air escape during material injection. Before fabrication, the mold components were coated with a release agent (Ease Release 200) and left to dry for 10 minutes. A silicone mixture made of polydimethylsiloxane (PDMS, Sylgard 184) and Ecoflex 00-10 (1:10 ratio, excluding the PDMS crosslinking agent) was prepared and degassed for 10 minutes. After assembling the mold, the material was injected initially into the pillar holes, then through the base holes to ensure complete filling of the empty cavity of the assembled mold. The material was left polymerizing at 50 °C for 1.5 hours, followed by 24 hours at room temperature before opening to retrieve the prototypes.

## Force measurement setup

The biohybrid actuator was positioned between two graphite electrodes inside a Petri dish. The Petri dish contained the two-post system in which the tissue was assembled and filled with a culture medium composed of DM supplemented with ACA. The bending of the two-post system induced by muscle contraction under electrical stimulation was recorded using the Leica Thunder imaging system, as shown in Fig. 3A.

The contraction force of the muscle actuators was analyzed following the protocol reported in Guix et al. and Mestre et al.[18,34,35].

The contracting muscle tissue exerts a force towards the two-post system, making them bent. Tissue contraction and consequent post-bending are recorded and then analyzed using a homemade Python script that calculates the post-border displacement observed in the video related to tissue contraction. The Euler-Bernoulli beam bending equation was used to estimate the contractile force from the post-discharge.

$$P = \frac{3EI_z y(a)}{a^3} \tag{5}$$

where $P$ is the applied force, $E$ is the Young's modulus of the PDMS post (206 kPa), $a$ is the height where the post-border displacement is being measured (being the z-axis position of the tissue in the post under evaluation, a value that can be taken from the meta-data of a z-stack taken from the tissue to the bottom of the post), $I_z$ is the second moment of area of the post around the z-axis, and y(a) is the displacement of the post obtained with Python. The second moment of area ($I_z$) around the z-axis of the post is a constant and follows the following equation:

$$I_z = \frac{w^3 L}{12} \tag{6}$$

where $w$ = 0.6 mm and $L$ = 3 mm are the lateral dimensions of the post base.

A case test of a BHM-based catheter device was performed using the setup shown in Fig. 3B. The biohybrid actuator was incorporated into a PDMS-compliant catheter prototype. The catheter prototype had on its top two pillars designed to position the actuator, allowing this way to induce a bending of the catheter depending on the contraction of the actuator. The bending profile was recorded using the Leica Thunder System as described above. The bending angle was obtained using a custom-made Python algorithm.

## Biohybrid actuator stimulation procedures

Four different stimulation strategies were carried out to verify the different capabilities of the biohybrid actuator and a prototype of BHM hosting the same actuator.

First, the capability to induce a repeatable biohybrid actuator contraction was verified. The contraction of the biohybrid actuator was tested using two different actuators and stimulating with a frequency of 1Hz. The first bioactuator was stimulated using four different waveforms (biphasic symmetric, biphasic asymmetric charge-balanced, monophasic, triangular biphasic charge-balanced) with 5 ms PW and 18 mA of amplitude. The second biohybrid actuator was subjected to biphasic symmetric stimuli with different PW (2 ms, 20 ms, 50 ms) to verify the effect of increasing the delivered charge during the stimulation task. Stimulation was performed using a train of stimuli of 1 Hz for 10 seconds.

Second, the capability to induce a biohybrid actuator contraction maintained over time, recreating muscle tetanic contraction, was tested. A biohybrid actuator was stimulated with a train of 50 Hz pulses for 10 seconds. Stimulation was performed using four different waveforms (biphasic symmetric, biphasic asymmetric charge-balanced, monophasic, and triangular biphasic charge-balanced) with 5 ms Pw and 19 mA of amplitude.

Third, the capability to dynamically modulate the contraction of the biohybrid actuator over time was also verified. Three biohybrid actuators were stimulated using a staircase-patterned linear amplitude algorithm. Stimulation was delivered in 11 steps of 2 seconds duration each. Stimulation amplitude was linearly modulated between steps starting from 3 mA to 18 mA. At each step, a train of 50 Hz biphasic symmetric pulses with a PW of 5 ms was delivered.

Finally, a preliminary application of the proposed electrical stimulator to control the movements of a BHM was investigated. A biohybrid actuator was embedded over a catheter prototype to induce the bending of the tip of a catheter. Two stimulation subtasks were performed to check the possibility of maintaining the catheter bent over time, using a train of 50Hz pulse and amplitude modulation to modify the catheter bending dynamically.

## Results and discussion

### Power consumption

The device's power consumption was measured to be 1 W during regular operation and reached a maximum power consumption of 1.3 W when all the high-voltage amplifiers were in saturation (90 V). The current absorbed during regular operation has been calculated at about 200 mA. Using a power bank for a smartphone with a capacity of 22,000 mAh, the working time of the device would be about 110 h in regular operation, and it would be 84 hours with all the stimulation channels active. To guarantee a working time of 12 h, it would be sufficient to have a small battery of about 3200 mAh.

### Twitch stimulation

The stimulation was carried out to induce a rapid, non-sustained contraction of the biohybrid actuator, corresponding to twitch contractions on different samples using trains of pulses with a frequency of 1 Hz for 10 s.

First, the effect of the waveform on the contraction performances at fixed amplitude (18 mA) and PW (2 ms) was tested (Fig. 4A). Although the contraction appears to be consistent with the timing induced by the stimulation, it can be seen how the contraction of the sample is affected by the type of waveform used during electrical stimulation, showing how the stimulator sample responds more decisively to the symmetrical biphasic stimulus. This difference in contraction is consistent with the total charge injection, as both the anodic and cathodic phases of the symmetric waveform can induce the cell action potential, thus allowing for increased recruitment of the fibers. Although a similar effect should also occur with the asymmetric biphasic form, the difference in amplitude between the anodic phase and the cathodic phase means that one of the two stimulation phases has a lower capacity to induce membrane depolarization, thus being less effective. Similar consideration can be done for the triangular waveform, in which the injected charge is half that of the rectangular shape.

Then, the influence of a PW was investigated using trains of symmetrical biphasic pulses of constant amplitude (15 mA) and different values of PW (2 ms, 20 ms, 50 ms). As can be seen from the graph in Fig.

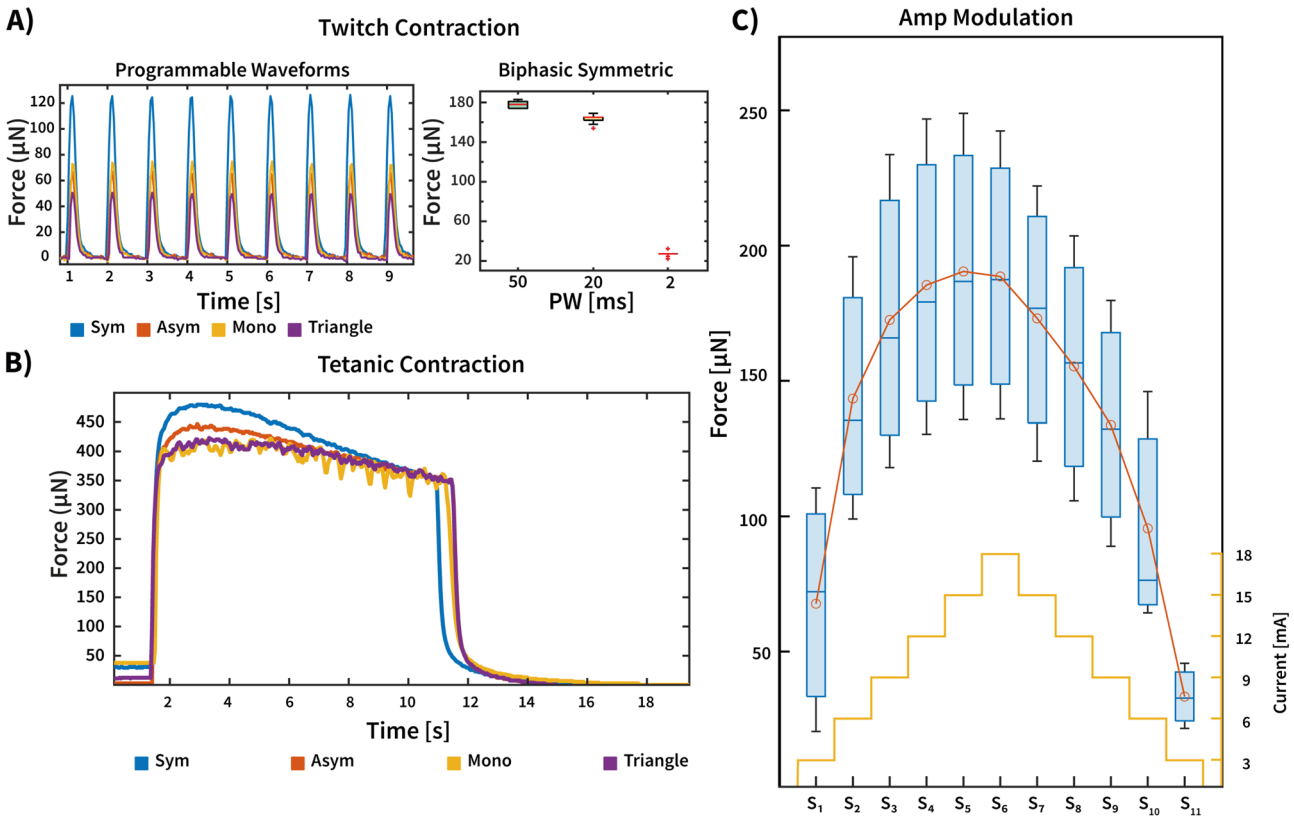


**Figure 4**. Twitch stimulation was performed using train of pulses with frequency of 1 Hz. The arbitrary waveform generation of the proposed device was used to verify the capability to induce twitch with different kind of stimulation waveforms. The pulse width programmability was investigated using biphasic symmetric waveforms, verifying the capability to modify the muscle tissue contraction (**A**). Tetanic stimulation was performed using a train of pulses with a frequency of 50 Hz. The arbitrary waveform generation of the proposed device was used to verify the capability to induce tetanic contraction with different kinds of stimulation waveforms (**B**). Modulation of biohybrid actuators contractions through amplitude modulation. A staircase modulation of 6 steps of same size from a minimum current of 3 mA to a maximum current of 18 mA. The box chart reports the average and standard variation of three independent experiments with three different biohybrid actuators (**C**).

4A, as the duration of stimulation increases, it is possible to modify the force of contraction of the tissues, as also previously reported in the literature[36]. The increase in injected charge due to longer stimulations has been reported to increase muscle fiber recruitment, resulting in a more significant tissue contraction.[19,37,38]

## Programmable tetanic contraction

Although the possibility of inducing twitch contraction in muscle tissue is a valuable benchmark for the biohybrid actuator stimulation strategy, their application in soft robotic applications generally involves more sophisticated functions. In particular, the capability to keep a contraction for a significant time, recreating tetanic contractions, is fundamental to enabling a given functionality (such as grasping or bending during movement). Moreover, the possibility of modulating the actual force has many important implications in the actual response of the soft robot: for instance, increasing the deformation without a complete reset of the stimuli, which would determine a complete relaxation of the robot shape. Additionally, this function enables the development of fully controllable soft robots through feedback systems. Indeed, the effect of a given stimulus in terms of actual force or realized deformation can be read by real-time force or bending sensors[39,40], and this information is used to adapt the amplitude of the stimulus for improved performances. Both features are strongly reliant on the capability of the stimulator to provide more sophisticated stimuli, having a high degree of programmability. First, a verification of the stimulation circuit performance in inducing tetanic contraction was investigated. Figure 4B reports experimental results obtained using different stimulation waveforms (biphasic symmetrical, asymmetric charge-balanced, monophasic waveforms, and biphasic triangular with balanced charge) in a 10 s train of pulses with a frequency of 50 Hz and an amplitude of 18 mA. Differently from what is obtained on twitch induction, the different stimulation modes induce a similar contraction, although the symmetric waveform has a higher contraction peak. It is noteworthy that the forces obtained in tetanic contractions are much higher than those previously obtained in twitch experiments. Aside from differences among different biohybrid actuators, the effect of frequency on muscle fiber recruitment has been thoroughly explained in the literature, showing how it is possible to increase the contraction force by increasing the stimulation frequency, both on humans[41] and on biohybrid actuators[42], thus providing a further demonstration of the correct functionality of the stimulation circuit.

It is possible to observe how the contraction force decreases as the time of inclusion passes, indicating a possible tissue relaxation effect. This effect could be due to the absence of dynamic perfusion inside the petri dish, resulting in an insufficient amount of calcium ions to maintain the contraction at maximum strength. However, to say this with certainty, it would be necessary to perform further electrophysiological analyses associated with the electrical inclusion.

Then, the possibility of dynamically modulating the contraction was demonstrated, exploiting the programmability of the circuit in terms of the amplitude of the stimuli. Amplitude modulation can represent a key modulation technique to dynamically modify the position of a biorobotic device, since the variations in amplitude can be exploited to vary the recruitment of the fibers in the biohybrid actuator, thus modifying the applied contraction force. Although amplitude modulation is a well-appreciated and documented technique in functional electrical stimulation (FES)[43,44] and in neural stimulation for sensory feedback[45,46], its applicability to biohybrid actuators has yet to be investigated in detail.

A stimulation pattern using symmetric biphasic PW stimuli of 5ms and 50 Hz frequency was employed to verify the possibility to dynamically control the fibers contraction in the biohybrid actuator. The amplitude was modified linearly including 11 steps long, starting from a minimum amplitude of 3 mA (step 1), reaching a maximum amplitude of 18 mA (step 6), and returning to the initial amplitude (step 11). Each stimulation step lasts 2 s, and the amplitude, frequency, and PW parameters do not vary within the step. Figure 4C shows average contraction during the stimulation steps of three different biohybrid actuators. Although a certain variability can be observed, as a consequence of the different force values available at each biohybrid actuator tested, a linear variation of the force with the amplitude of the stimulation current is clearly observed. This results supports amplitude modulation as a valuable approach to modifying the recruitment of the muscle tissue's fibers to induce different behaviors in the biohybrid actuator.

## Application of biohybrid actuator stimulation in a BHM

To demonstrate the feasibility of the proposed approach to the actual control of a BHM, the investigated biohybrid actuator was integrated into a BHM demonstrator, consisting of a PDMS-based catheter tip containing two pillars for holding the biohybrid actuator[47,48].

The BHM system (from now on, biohybrid catheter) was tested under two conditions: in the first, a tetanic contraction was induced to demonstrate the capability of the stimulation system to induce a prolonged bending in the catheter tip, In the second condition, the amplitude modulation strategy was tested to verify the possibility of adjusting the catheter tip's bending by modulating the biohybrid actuator's contraction. Both features are fundamental for the development of a biohybrid catheter with remote deformation control. Indeed, keeping a given bending is important to ensure the correct catheter motility in the bloodstream, particularly when strict bifurcations are encountered, thus allowing a reduced risk of impact with the blood vessel walls and a risk for hemorrhage.

Figure 5 reports the results of the experiments carried out on the biohybrid catheter. In tetanic contraction (Fig. 5A) applied to the catheter as the recorded bending angle (calculated between the fixed part of the tip and the bent section) in real-time, extracted by means of a custom Python script from video taken by a Leica Thunder System **(Video S1 in Supporting Information)**. The bending was obtained by applying a train of pulses of a frequency of 50 Hz, PW 5 ms, and amplitude 18 mA. A bending angle of about $0.9^{\circ}$ was obtained in this condition, which was well kept for the whole duration of the experiment with a limited variability (not exceeding the 20%).

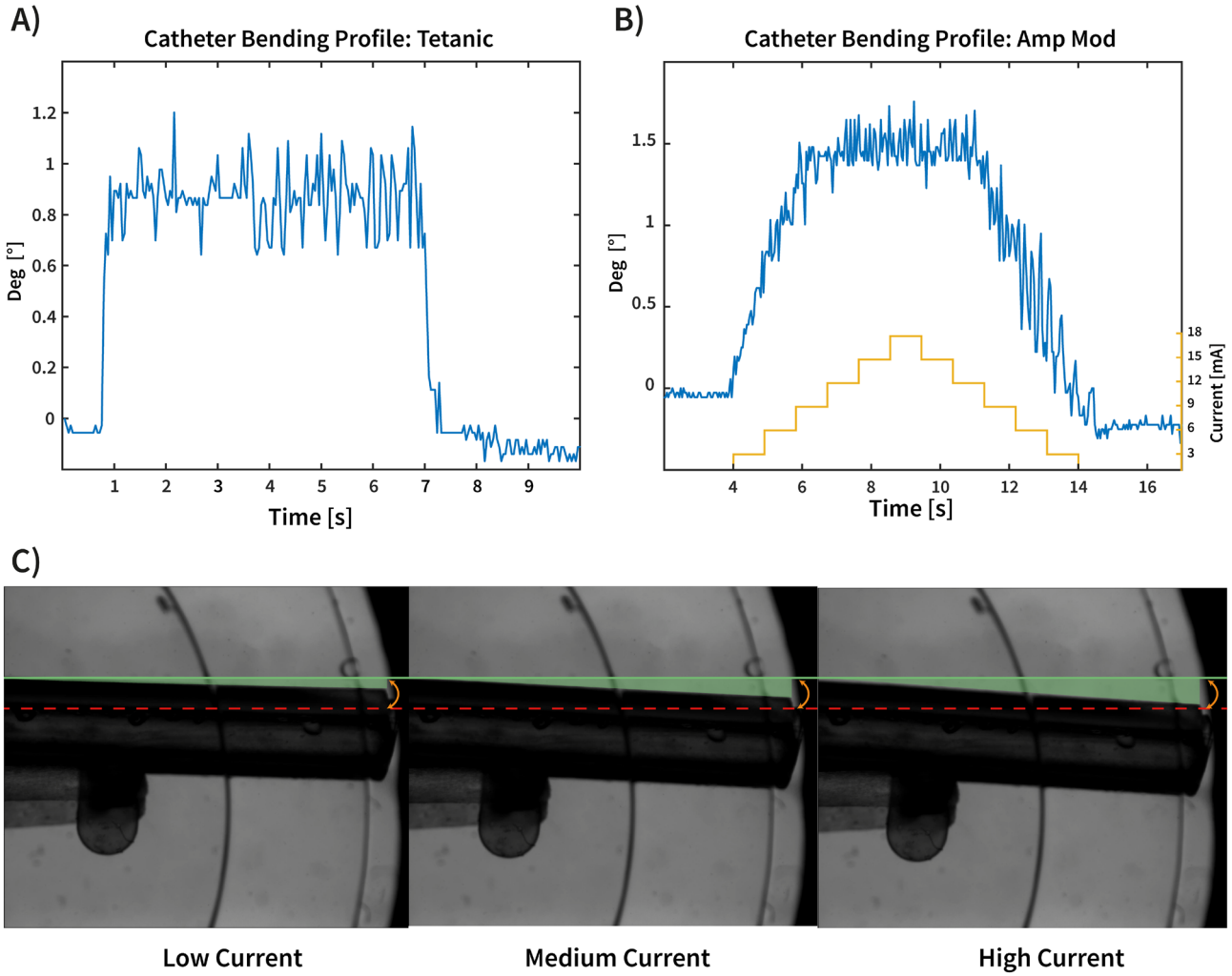


**Figure 5**. Biohybrid driven catheter stimulation. The catheter was stimulated using a train of pulses with a frequency of 50 Hz, amplitude of 18 mA, and pulse width 5ms to verify the capability to induce stable bending of the catheter (**A**). Amplitude modulation was performed to verify the capability to dynamically modify the bending of the catheter (**B**). Catheter bending (**C**).

Figure 5B reports an example of dynamic bending in the catheter tip by amplitude modulation, displaying the bending angle variation in real time **(from Video S2 in Supporting Information)**. Stimulation was performed as follows. The amplitude was modified linearly 11 steps long, starting from a minimum amplitude of 3 mA (step 1), reaching a maximum amplitude of 18 mA (step 6), and returning to the initial amplitude (step 11). Modular increase in catheter bending is displayed until the maximum bending reach (up to 1.5 °), as well as subsequent gradual relaxation until the end of stimulation. In this case, the different bending angles obtained at different amplitudes of the stimuli are hard to be defined as a consequence of the significant noise, mostly related to the resolution of the recognition system and of the script employed for the bending angle extrapolation. It is important to highlight that the tested catheter is a benchmark for the stimulation strategy, thus being not optimized for any specific applications: the obtained performances represent a proof-of-concept application of the stimulation circuits and its potentialities, thus allowing foreseeing future enhancement with refined BHMs.

## Conclusions

This paper reports the development of a custom, portable stimulation system that can be used to develop and investigate control techniques for BHMs. The device implements an innovative approach to BHM stimulation, based on a CCM instead of the typical VCM, to obtain better control over muscle tissue contraction and reduce the risk of stress and failure of the biohybrid actuator. Moreover, the system implements a high degree of programmability in terms of stimulation patterns, including different default waveforms that can be modified in amplitude, pulse width, and frequency through a user-friendly GUI. The high voltage compliance (± 90 V) allows adaptation to various load impedances, guaranteeing a stimulation of 18 mA up to impedances of 5 kΩ. The device was tested using biohybrid actuators, showing the possibility of controlling their twitch or inducing tetanic contraction. Furthermore, through amplitude modulation, the device has been shown to be

capable of affecting the contraction force of the tissues used, allowing the elicited contraction force to increase or decrease. Finally, the use of the stimulation circuit for the control of a prototype of a BHM catheter was explored, providing a preliminary feasibility demonstration in the induction and maintenance of bending and its dynamic modulation. It is important to underline that both biohybrid actuators and biohybrid machines must be considered as a benchmark for stimulation strategy validation, i.e., without targeting a specific final performance in terms of contraction ability. Indeed, to this aim, BHM must be designed to fit a specific application scenario: at this stage, this aspect has been not yet defined, and will be faced in future research activities However, the results reported demonstrate that the proposed approach may significantly improve soft robotic control toward the exploitation of even more refined BHMs, including a closed-loop system that integrates sensors for real-time monitoring of the biohybrid actuator functionality.

## Data availability

All data generated or analyzed during the study are included in the manuscript. Data are available from the corresponding author upon reasonable request.

Received: 24 February 2025; Accepted: 9 June 2025
Published online: 02 July 2025

## References

1. Ricotti, L. & Menciassi, A. Bio-hybrid muscle cell-based actuators. *Biomed. Microdevice* **14**, 987–998 (2012).
2. Ricotti, L. et al. Biohybrid actuators for robotics: A review of devices actuated by living cells. *Sci. Robot.* **2**, eaaq0495 (2017).
3. Carlsen, R., Edwards, M., Zhuang, J., Pacoret, C. & Sitti, M. Magnetic steering control of multi-cellular bio-hybrid microswimmers. *Lab Chip* **14**, 3850–3859. https://doi.org/10.1039/C4LC00707G (2014).
4. Asano, T., Ishizua, T. & Yawo, H. Optically controlled contraction of photosensitive skeletal muscle cells. *Biotechnol. Bioeng.* **109**, 199–204 (2012).
5. Raman, R. et al. Optogenetic skeletal muscle-powered adaptive biological machines. *Proc. Natl. Acad. Sci.* **113**, 3497–3502. https://doi.org/10.1073/pnas.1516139113 (2016).
6. Sun, L. et al. Biohybrid robotics with living cell actuation. *Chem. Soc. Rev.* **49**, 4043–4069. https://doi.org/10.1039/D0CS00120A (2020).
7. Dennis, R. & Kosnik, P. Excitability and isometric contractile properties of mammalian skeletal muscle constructs engineered in vitro. *In Vitro Cellular & Developmental Biology - Animal.***36**, 327–335 (2000).
8. Filippi, M., Balciunaite, A., Georgopoulou, A., Paniagua, P., Drescher, F., Nie, M., Takeuchi, S., Clemens, F. & Katzschmann, R. Sensor-Embedded Muscle for Closed-Loop Controllable Actuation in Proprioceptive Biohybrid Robots. *Adv. Intell. Syst*. 2400413. https://doi.org/10.1002/aisy.202400413.
9. Xu, H. et al. Sperm-Hybrid Micromotor for Targeted Drug Delivery. *ACS Nano* **12**, 327–337. https://doi.org/10.1021/acsnano.7b06398 (2018).
10. Stanton, M. et al. Biohybrid microtube swimmers driven by single captured bacteria. *Small* **13**, 1603679 (2017).
11. Sun, L. et al. Biohybrid robotics with living cell actuation. *Chem. Soc. Rev.* **49**, 4043–4069 (2020).
12. Kim, Y. et al. Remote control of muscle-driven miniature robots with battery-free wireless optoelectronics. *Sci. Robot.* **8**, eadd1053. https://doi.org/10.1126/scirobotics.add1053 (2023).
13. Sakar, M. et al. Formation and optogenetic control of engineered 3D skeletal muscle bioactuators. *Lab Chip* **12**, 4976–4985. https://doi.org/10.1039/C2LC40338B (2012).
14. Park, S. et al. Phototactic guidance of a tissue-engineered soft-robotic ray. *Science* **353**, 158–162. https://doi.org/10.1126/science.aaf4292 (2016).
15. Carlsen, R. & Sitti, M. Bio-Hybrid Cell-Based Actuators for Microsystems. *Small* **10**, 3831–3851 (2014).
16. Cvetkovic, C. et al. Three-dimensionally printed biological machines powered by skeletal muscle. *Proc. Natl. Acad. Sci.* **111**, 10125–10130. https://doi.org/10.1073/pnas.1401577111 (2014).
17. Pagan-Diaz, G. et al. Simulation and Fabrication of Stronger, Larger, and Faster Walking Biohybrid Machines. *Adv. Func. Mater.* **28**, 1801145. https://doi.org/10.1002/adfm.201801145 (2018).
18. Guix, M. et al. Biohybrid soft robots with self-stimulating skeletons. *Sci. Robot.* **6**, eabe7577 (2021).
19. Merrill, D., Bikson, M. & Jefferys, J. Electrical stimulation of excitable tissue: design of efficacious and safe protocols. *J. Neurosci. Methods* **141**, 171–198 (2005).
20. Bisoni, L., Carboni, C., Raffo, L., Carta, N. & Barbaro, M. An HV-CMOS integrated circuit for neural stimulation in prosthetic applications. *IEEE Trans. Circ. Syst. II Express Briefs.* **62**, 184–188 (2015).
21. Cornman, J., Akhtar, A. & Bretl, T. A portable, arbitrary waveform, multichannel constant current electrotactile stimulator. *2017 8th International IEEE/EMBS Conference On Neural Engineering (NER)*. pp. 300-303 (2017)
22. Trout, M., Harrison, A., Brinton, M. & George, J. A portable, programmable, multichannel stimulator with high compliance voltage for noninvasive neural stimulation of motor and sensory nerves in humans. *Sci. Rep.* **13**, 3469. https://doi.org/10.1038/s41598-023-30545-8 (2023).
23. Collu, R. et al. Wearable High Voltage Compliant Current Stimulator for Restoring Sensory Feedback. *Micromachines*. **14**, 782 (2023).
24. Collu, R., Earley, E., Barbaro, M. & Ortiz-Catalan, M. Non-rectangular neurostimulation waveforms elicit varied sensation quality and perceptive fields on the hand. *Sci. Rep.* **13**, 1588 (2023).
25. Zhang, M., Tang, Z., Liu, X. & Van der Spiegel, J. Electronic neural interfaces. *Nature Electronics.* **3**, 191–200. https://doi.org/10.1038/s41928-020-0390-3 (2020).
26. Akiyama, Y., Nakayama, A., Nakano, S., Amiya, R. & Jun Hirose. An Electrical Stimulation Culture System for Daily Maintenance-Free Muscle Tissue Production. *Cyborg Bionic Syst*. **2021** (2021).
27. Ahmed, R. & Reifsnider, K. Study of Influence of Electrode Geometry on Impedance Spectroscopy. https://doi.org/10.1115/FuelCell2010-33209 (2010).
28. Ruiz, G. & Felice, C. Non-linear response of an electrode–electrolyte interface impedance with the frequency. *Chaos, Solitons & Fractals*. **31**, 327–335 (2007).
29. Tamura, Y., Kouzaki, K., Kotani, T. & Nakazato, K. Electrically stimulated contractile activity-induced transcriptomic responses and metabolic remodeling in C2C12 myotubes: twitch vs. tetanic contractions. *Am. J. Physiol. Cell Physiol.* **319**, C1029–C1044 (2020).
30. Hamaguchi, H. et al. Establishment of a system evaluating the contractile force of electrically stimulated myotubes from wrinkles formed on elastic substrate. *Sci. Rep.* **12**, 13818. https://doi.org/10.1038/s41598-022-17548-7 (2022).
31. Pasluosta, C., Kiele, P. & Stieglitz, T. Paradigms for restoration of somatosensory feedback via stimulation of the peripheral nervous system. *Clin. Neurophysiol.* **129**, 851–862 (2018).

32. Yuan, Y., Zheng, L., Feng, Z. & Yang, G. Different effects of monophasic pulses and biphasic pulses applied by a bipolar stimulation electrode in the rat hippocampal CA1 region. *Biomed. Eng. Online* **20**, 1–12 (2021).
33. Piallat, B. et al. Monophasic but not biphasic pulses induce brain tissue damage during monopolar high-frequency deep brain stimulation. *Neurosurgery* **64**, 156–163 (2009).
34. Mestre, R. et al. Force modulation and adaptability of 3D-bioprinted biological actuators based on skeletal muscle tissue. *Adv. Mater. Technol.* **4**, 1800631 (2019).
35. Mestre, R. et al. Improved Performance of Biohybrid Muscle-Based Bio-Bots Doped with Piezoelectric Boron Nitride Nanotubes. *Adv. Mater. Technol.* **8**, 2200505. https://doi.org/10.1002/admt.202200505 (2023).
36. Gorman, P. & Mortimer, J. The Effect of Stimulus Parameters on the Recruitment Characteristics of Direct Nerve Stimulation. *IEEE Trans. Biomed. Eng.* **BME–30**, 407–414 (1983).
37. Brummer, S. & Turner, M. Electrical stimulation of the nervous system: The principle of safe charge injection with noble metal electrodes. *Bioelectrochem. Bioenerg.* **2**, 13–25 (1975).
38. Mortimer, J., Kaufman, D. & Roessmann, U. Intramuscular electrical stimulation: Tissue damage. *Ann. Biomed. Eng.* **8**, 235–244. https://doi.org/10.1007/BF02364479 (1980).
39. Lai, S., Fuentes, J., Guix, M., Casula, G., Cosseddu, P. & Sánchez, S. Real-Time Force Monitoring of Electrically Stimulated 3D-Bioengineered Muscle Bioactuators Using Organic Sensors with Tunable Sensitivity. *Adv. Intell. Syst*. 2400407. https://doi.org/10.1002/aisy.202400407.
40. Zhao, H. et al. Rogers Compliant 3D frameworks instrumented with strain sensors for characterization of millimeter-scale engineered muscle tissues. *Proc. Natl. Acad. Sci.* **118**, e2100077118. https://doi.org/10.1073/pnas.2100077118 (2021).
41. Kesar, T., Chou, L. & Binder-Macleod, S. Effects of stimulation frequency versus pulse duration modulation on muscle fatigue. *J. Electromyogr. Kinesiol.* **18**, 662–671 (2008).
42. Morimoto, Y., Onoe, H. & Shoji, T. Biohybrid robot powered by an antagonistic pair of skeletal muscle tissues. *Sci. Robot.* **3**, eaat4440. https://doi.org/10.1126/scirobotics.aat4440 (2018).
43. Lynch, C. & Popovic, M. Functional electrical stimulation. *IEEE Control Syst. Mag.* **28**, 40–50 (2008).
44. Braz, G., Russold, M. & Davis, G. Functional electrical stimulation control of standing and stepping after spinal cord injury: a review of technical characteristics. *Neuromodul. Technol. Neural Interface.* **12**, 180–190 (2009).
45. Valle, G. et al. Biomimetic intraneural sensory feedback enhances sensation naturalness, tactile sensitivity, and manual dexterity in a bidirectional prosthesis. *Neuron* **100**, 37-45.e7 (2018).
46. Valle, G. et al. Comparison of linear frequency and amplitude modulation for intraneural sensory feedback in bidirectional hand prostheses. *Sci. Rep.* **8**, 16666. https://doi.org/10.1038/s41598-018-34910-w (2018).
47. Salvatori, C., Trucco, D., Niosi, I., Ricotti, L. & Vannozzi, L. A Novel Steerable Catheter Controlled with a Biohybrid Actuator: A Feasibility Study. *Biomimetic Biohybrid Syst* 378–393 (2023).
48. Bartolucci, A., Fuentes, J., Guarnera, D., Lezcano, F., Crespo-Cuadrado, M., Guachi-Guachi, L., Iacoponi, F., Salvatori, C., Collu, R., Barbaro, M., Lai, S., Ricotti, L., Sánchez, S. & Vannozzi, L. Monolithic Biohybrid Flexure Mechanism Actuated by Bioengineered Skeletal Muscle Tissue. *Adv. Intell. Syst*. 2400989. https://doi.org/10.1002/aisy.202400989.


## Acknowledgements

This project has received funding from the European Union's Horizon Europe research and innovation programme under grant agreement No. 101070328. Views and opinions expressed are however those of the authors only and do not necessarily reflect those of the European Union or European Commission. Neither the European Union nor the granting authority can be held responsible for them. CERCA program by the Generalitat de Catalunya, the Secretaria d'Universitats i Recerca del Departament d'Empresa i Coneixement de la Generalitat de Catalunya through the project 2021 SGR 01606, and the "Centro de Excelencia Severo Ochoa", funded by Agencia Estatal de Investigación (CEX2018-000789-S).

## Author contributions

R.C. developed the electrical stimulator and designed the tests. J.F. developed the biohibrid actuators. R.C., J.F., F.L., M.C.C., and A.B. executed the experiments. J.F., F.L., M.C.C. prepared the setup and elaborated the data. A.B. designed and developed the catheter. S.S., L.R., L.V., S.L., and M.B. supervised the experiments. R.C. and S.L. drafted the manuscript. All the authors reviewed and approved the submitted manuscript.

## Declarations

## Competing interests

The authors declare no competing interests.

## Additional information

**Supplementary Information** The online version contains supplementary material available at https://doi.org/10.1038/s41598-025-06465-0.

**Correspondence** and requests for materials should be addressed to R.C.

**Reprints and permissions information** is available at www.nature.com/reprints.

**Publisher's note** Springer Nature remains neutral with regard to jurisdictional claims in published maps and institutional affiliations.